applied sciences

MDPI

Article

Anti-Inflammatory Flavonolignans from *Triticum aestivum* Linn. Hull

Ah-Reum Han [1,†], Yun-Seo Kil [2,†], Min Jeong Hong [1], Jisu Park [1], Hyeon Hwa Park [1], Chang Hyun Jin [1], Joo-Won Nam [2,*] and Jin-Baek Kim [1,*]

1 Advanced Radiation Technology Institute, Korea Atomic Energy Research Institute, Jeollabuk-do, Jeongeup-si 56212, Korea; arhan@kaeri.re.kr (A.-R.H.); hongmj@kaeri.re.kr (M.J.H.); parksj94@kaeri.re.kr (J.P.); hhp856@kaeri.re.kr (H.H.P.); chjin@kaeri.re.kr (C.H.J.)

2 College of Pharmacy, Yeungnam University, Gyeongsangbuk-do, Gyeongsan-si 38541, Korea; yskil@yu.ac.kr

* Correspondence: jwnam@yu.ac.kr (J.-W.N.); jbkim74@kaeri.re.kr (J.-B.K.); Tel.: +82-53-810-2818 (J.-W.N.); +82-63-570-3313 (J.-B.K.)

† These authors contributed equally to this work.

Received: 30 October 2020; Accepted: 2 December 2020; Published: 4 December 2020

Abstract: Wheat (*Triticum aestivum* Linn.; Poaceae) is a very common and important food grain and ranks second in total cereal crop production. A large amount of wheat hull is produced after threshing that, as the non-food part of wheat, is agro-waste, accounting for 15~20% of the wheat. This study aimed at biologically and phytochemically investigating wheat hull for its valorization as a by-product. In our ongoing search for natural product-derived anti-inflammatory agents, *T. aestivum* hull was evaluated for its nitric oxide (NO) production inhibition in lipopolysaccharide (LPS)-activated RAW 264.7 cells, and the phytochemical investigation of the ethyl acetate fraction showing inhibitory effect led to the isolation of a flavone (**1**) and seven flavonolignans (**2**–**8**). Compounds **2**–**8** have not yet been isolated from *Triticum* species. All compounds were evaluated for their LPS-induced NO production inhibition, and **1**, **2**, **4**, **6**, and **8** exhibited inhibitory effects with IC_{50} values ranging from 24.14 to 58.95 μM. These results suggest the potential of using *T. aestivum* hull as a source for producing anti-inflammatory components, enhancing its valorization as a by-product.

Keywords: *Triticum aestivum*; Poaceae; flavonolignan; anti-inflammation

1. Introduction

Wheat (*Triticum aestivum* Linn.) is one of the world's most produced and consumed major food crops and its products are primary diet components, affecting human health directly [1]. It is generally cultivated for its grains used for flour production. Its products exhibit high carbohydrate content, providing energy, and are reach in nutrients, including protein, minerals, vitamins, fibers, and bioactive components [2]. In addition, improved varieties of wheat have been steadily developed with a focus on the high functionality of wheat, such as colored wheat grains having a broad range of colors from red to purple with greater antioxidant activity [3]. An interest in the health benefits of whole grain or wheat bran obtained by milling has been increasing in recent years, and several studies have been reported that whole grain or bran of wheat is helpful in improving health and preventing various diseases such as diabetes, cancer, and allergies [4–8]. However, there are few reports on the phytochemical and biological study of agro-industrial waste produced after threshing wheat, such as the hull (including spike) and straw. These wheat by-products have been traditionally used as animal feed sources, fuel in the livestock industry, and were studied as wood fiber alternatives [9]. Several studies indicated that wheat parts other than the grain are also rich in pharmacological ingredients [10–15]. Flavone glycosides and phenolic acids found in its aerial parts showed DPPH free radical scavenging

activities [10]. Constituents of its bran or hull were reported to have anticancer activities, for example, oxyphytosterols in its brans induced human colon cancer cell death through the apoptosis pathway [11] and tricin, a major flavone in its hull, was cytotoxic against hepatic and pancreatic cancer cell lines with no effects on normal cell lines [12]. 5-Alk(en)ylresorcinols, aliphatic compounds, and phenolic glycoside found in wheat bran showed anti-allergic activities [8,13]. Glycolipids and flavonoids isolated from its sprouts inhibited adipogenesis in 3T3-L1 preadipocytes [14,15]. A summary of the isolates previously reported from various parts of wheat is presented in Table S1 and Figure S1 (Supplementary Materials).

Nitric oxide (NO) is a free radical, widely distributed in the body, that regulates various biological functions such as vasodilation, smooth muscle contraction, nerve signal transmission, platelet aggregation inhibition, and immune regulation. It is involved in anticancer, antibacterial, and various inflammatory reactions, and maintains homeostasis [16]. However, if NO is excessively produced, it may cause conditions such as inflammatory reaction hyperactivity and the acceleration of malignant processes [17,18]. NO synthase (NOS), an enzyme that generates NO using L-arginine as a substrate, could be broadly classified as constitutive NOS (cNOS) and inducible NOS (iNOS). cNOS exhibits an endothelial isoform (eNOS) and a neuronal isoform (nNOS)—eNOS is present in vascular endothelial cells and nNOS is found in the nervous system, pancreatic β-islet cells and bronchi, and gastrointestinal endothelial cells [19,20]. cNOS expression is controlled by intracellular calcium ion (Ca^{2+}) and calmodulin concentrations, whereas iNOS is induced by proinflammatory cytokines, such as lipopolysaccharide (LPS), interferon-γ, interleukin-1, and tumor necrosis factor-α, independently from the cellular Ca^{2+} concentration [20–22]. Therefore, the inhibition of LPS-induced NO production is considered as an iNOS inhibitory process in inflammation and carcinogenesis [23].

In our ongoing research program to find the bioactive compounds from natural sources, a methanol extract as well as *n*-hexane, ethyl acetate, and *n*-butanol-soluble fractions of *T. aestivum* hull were tested for NO production inhibitory activity in LPS-activated RAW 264.7 macrophage cells. The ethyl acetate fraction showed potent inhibition with 62.11% at 50 μg/mL. Through a detailed phytochemical investigation on this active fraction, we isolated and identified eight compounds, including flavone (**1**) and flavonolignans (**2**–**8**). In this study, we describe the isolation, structural identification, and biological results of these compounds and chemotaxonomy significance.

2. Materials and Methods

2.1. General Information

The optical rotation was measured on a JASCO DIP-1000 polarimeter (JASCO Co., Tokyo, Japan). Before use, the polarimeter was tested with an aqueous solution of D-glucose (Sigma-Aldrich, St. Louis, MO, USA). when in equilibrium with a stable ratio of α/β-isomers. Samples were dissolved in methanol for the optical rotation measurements and the concentration was described in g/100 mL. The circular dichroism (CD) measurement was performed for each sample in methanol using a JASCO J-810 CD-ORD spectropolarimeter (JASCO Co., Tokyo, Japan). The CD curves were obtained in a range of 200-400 nm wavelength by 5-fold of accumulation (scanning speed, 100 nm/min; response, 2 s). The NMR experiments were performed on a 600 MHz Varian NMR spectrometer (VNS-600, Palo Alto, CA, USA) and a JNM-ECA 500 MHz NMR instrument (JEOL Ltd., Tokyo, Japan). The acquired ^{1}H and ^{13}C NMR data were referenced to δ_H 3.31/δ_c 49.15 (for methanol-d_4 and 1:1 ratio of methanol-d_4 and acetone-d_6) and 2.05/29.92 (for acetone-d_6), respectively, and further processed using MestReNova 12.0.1 software (Mestrelab Research SL, Santiago de Compostela, Spain). LR-ESIMS was carried out on an Agilent 6120 series LC–MS system (Agilent Technologies, Santa Clara, CA, USA), equipped with a Luna C18(2) column (3 μm, 150 mm × 4.6 mm i.d., Phenomenex, Torrance, CA, USA). Samples of 0.1 mg/mL in methanol were analyzed, respectively, for 19 min in a gradient solvent system of 5% acetonitrile in water containing 0.05% formic acid and acetonitrile containing 0.05% formic acid at a flow rate of 0.7 mL/min. Mass data were collected over a scan mass range of 100–1000 amu in positive mode. An RP-18 (YMC gel ODS-A, 12 nm, S-75 μm, YMC Co., Kyoto, Japan) was used for column

chromatography (CC). The thin-layer chromatographic (TLC) analysis was performed on a Kieselgel 60 F_{254} (Merck, Darmstadt, Germany) and a Kieselgel 60 RP-18-F_{254S} device (Merck, Darmstadt, Germany), with visualization under UV light (254 and 365 nm) and by heating at 180 °C for 2 min after spraying 10% (*v*/*v*) sulfuric acid. A YMC-Pack ODS-AQ column (5 μm, 250 mm × 20 mm i.d., YMC Co., Tokyo, Japan) and a ChiralPak IF (5 μm, 250 mm × 4.6 mm i.d., Daicel Co., Osaka, Japan) were used for preparative high-performance liquid chromatography (HPLC) that was conducted on a Waters HPLC system (Waters Co., Milford, CT, USA). The medium-pressure liquid chromatography (MPLC) was performed on a CombiFlash Rf200 system (Teledyne ISCO, Lincoln, NE, USA) with RediSep Rf Normal Phase Silica columns. Dulbecco's modified Eagle's medium (DMEM), fetal bovine serum (FBS), and penicillin-streptomycin were purchased from Hyclone (Logan, UT, USA). LPS, dimethyl sulfoxide (DMSO), Griess reagent, and N^G-monomethyl-L-arginine acetate salt (L-NMMA) were purchased from Sigma-Aldrich (St. Louis, MO, USA). All other chemicals and solvents used in this study were of analytical grade.

2.2. Plant Material

Seeds of *T. aestivum* was sown and grown in constant soil conditions of the experimental field situated at 35.5699°N latitude by 126.9722°E longitude, at the Advanced Radiation Technology Institute, Korea Atomic Energy Research Institute (Jeongeup-si, Jeollabuk-do 56212, Korea). Spikes were labeled at flowering time and were harvested at 50 days after flowering (July 2017). This plant was bred and identified by Jin-Baek Kim and Min Jeong Hong, co-authors of this study. The remaining hull after threshing was collected and dried for further investigation. The voucher specimens (no. RB014) were deposited at the Advanced Radiation Technology Institute, Korea Atomic Energy Research Institute.

2.3. Extract and Isolation

The *T. aestivum* hull was dried and weighed 4 kg after drying. The dried sample was extracted with methanol (3 × 10 L) for 24 h at room temperature. The solvent was evaporated in vacuo to produce a methanol extract (79.2 g). It was dissolved in distilled water (2 L) and partitioned with *n*-hexane (3 × 2 L), ethyl acetate (3 × 2 L), and *n*-butanol (3 × 2 L), sequentially. Each solvent fraction was evaporated in vacuo to obtain fractions of *n*-hexane (10.8 g), ethyl acetate (9.2 g), and *n*-butanol (10.6 g). The ethyl acetate fraction was subjected to reversed-phase column chromatography (methanol/water, 1:1 to 9:1, *v*/*v*) to yield 10 fractions (F01–F10). Fraction F3 (310 mg) was chromatographed on a Sephadex LH-20 using 100% methanol, resulting in the isolation of **1** (5.5 mg). Fraction F04 (1.2 g) was subjected to MPLC (40 g HP Silica; *n*-hexane/ethyl acetate; 0–100 min, 9:1 to 15:85; 100–180 min, 15:85 to 0:1, 30 mL/min) to obtain subfractions F4-1-F4-10. Subfraction F4-8 (50 mg) was separated by HPLC (acetonitrile/formic acid (0.1%) in water, 45:55, 4 mL/min) to yield **7** (1.4 mg, t_R 44.9 min), **5** (2.3 mg, t_R 47.0 min), **6** (2.4 mg, t_R 50.4 min), **4** (2.0 mg, t_R 53.3 min), and a mixture fraction at t_R 49.3 min. Further purification of the mixture fraction using HPLC (acetonitrile/formic acid (0.1%) in water, 45:55, 1 mL/min) provided **8** (0.5 mg, t_R 28.6 min). Fraction F5 (500 mg) was subjected to MPLC (12 g HP Silica; *n*-hexane/ethyl acetate; 0–20 min, 1:0 to 4:1; 20–50 min, 4:1 to 1:1; 50–60 min, 1:1 to 0:1, 30 mL/min) to obtain subfractions F5-1-F5-11. The combined subfractions F5-7 and F5-8 (20 mg) were subjected to HPLC (acetonitrile/formic acid (0.1%) in water, 1:1, 4 mL/min), resulting in the isolation of **2** (1.5 mg, t_R 30.9 min) and **3** (2.6 mg, t_R 32.2 min).

Tricin (**1**): Yellow powder. ^{1}H NMR spectrum (600 MHz, methanol-d_4/acetone-d_6, 1:1), see Figure S2. LR-ESIMS (positive ions) *m*/*z* 331.1 $[M + H]^+$.

Tricin 4′-*O*-[*threo*-*β*-guaiacyl-(7″-*O*-methyl-9″-*O*-acetyl)-glyceryl] ether (**2**): Brown solid. $[\alpha]_D^{20}$ − 1.1° (*c* 0.1, methanol). ^{1}H (600 MHz, methanol-d_4 and acetone-d_6) and ^{13}C (150 MHz, methanol-d_4) NMR spectra, see Figures S3–S5. LR-ESIMS (positive ions) *m*/*z* 583.2 $[M + H]^+$.

Tricin 4′-*O*-[*erythro*-*β*-guaiacyl-(7″-*O*-methyl-9″-*O*-acetyl)-glyceryl] ether (**3**): Brown solid. $[\alpha]_D^{20}$ + 1.2° (*c* 0.1, methanol). ^{1}H (600 MHz, methanol-d_4 and acetone-d_6) and ^{13}C (150 MHz, methanol-d_4) NMR spectra, see Figures S3, S4, and S6. LR-ESIMS (positive ions) *m*/*z* 583.2 $[M + H]^+$.

Tricin 4′-*O*-[*threo*-*β*-guaiacyl-(9″-*O*-acetyl)-glyceryl] ether (**4**): Brown solid. $[\alpha]_D^{20}$ + 5.3° (*c* 0.1, methanol). ^{1}H (600 MHz, methanol-d_4 and acetone-d_6) and ^{13}C (150 MHz, methanol-d_4) NMR spectra, see Figures S7 and S8. LR-ESIMS (positive ions) *m*/*z* 569.2 $[M + H]^+$.

Tricin 4′-*O*-[*threo*-*β*-guaiacyl-(7″-*O*-methyl)-glyceryl] ether (**5**): Brown solid. $[\alpha]_D^{20}$−1.6° (*c* 0.1, methanol). ^{1}H (600 MHz, methanol-d_4 and acetone-d_6) and ^{13}C (150 MHz, methanol-d_4) NMR spectra, see Figures S9–S11. LR-ESIMS (positive ions) *m*/*z* 541.2 $[M + H]^+$.

Tricin 4′-*O*-[*erythro*-*β*-guaiacyl-(7″-*O*-methyl)-glyceryl] ether (**6**): Brown solid. $[\alpha]_D^{20}$ + 1.3° (*c* 0.1, methanol). ^{1}H (600 MHz, methanol-d_4 and acetone-d_6) and ^{13}C (150 MHz, methanol-d_4) NMR spectra, see Figures S9, S10, and S12. LR-ESIMS (positive ions) *m*/*z* 541.2 $[M + H]^+$.

Tricin 4′-*O*-[*threo*-*β*-4″-hydroxyphenyl-(7″-*O*-methyl)-glyceryl] ether (**7**): Brown solid. $[\alpha]_D^{20}$ + 4.0° (*c* 0.1, methanol). ^{1}H (600 MHz, methanol-d_4 and acetone-d_6) and ^{13}C (150 MHz, acetone-d_6) NMR spectra, see Figures S13–S15. LR-ESIMS (positive ions) *m*/*z* 511.2 $[M + H]^+$.

Tricin 4′-*O*-[*erythro*-*β*-4″-hydroxyphenyl-(7″-*O*-methyl)-glyceryl] ether (**8**): Brown solid. $[\alpha]_D^{20}$ + 10.9° (*c* 0.1, methanol). ^{1}H (600 MHz, methanol-d_4 and acetone-d_6) and ^{13}C (150 MHz, acetone-d_6) NMR spectra, see Figures S13, S14, and S16. LR-ESIMS (positive ions) *m*/*z* 511.2 $[M + H]^+$.

2.4. Measurement of NO Production on LPS-Stimulated RAW 264.7 Cells

NO production was measured in cultured RAW 264.7 macrophage cells. These cells were maintained in DMEM, supplemented with 10% FBS, 100 U/mL penicillin, and 100 μg/mL streptomycin, at 37 °C in a 5% CO_2 incubator. The cells were seeded into 96-well plates at a density of 2×10^5 cells/mL, then incubated at 37 °C for 24 h. The cells were pretreated for 2 h with various concentrations of compounds **1**–**3** and **5**–**8** (20, 30, and 40 μM) and compound **4** (10, 20, and 40 μM). Then, the cells were stimulated for 18 h in the medium with 1 μg/mL of LPS. The nitrite concentration in the media was measured by the Griess reaction. Standard sodium nitrite solutions were prepared and a 100 μL portion of Griess reagent {0.1% *N*-(1-naphthyl)ethylenediamine dihydrochloride in H_2O and 1% sulfanilamide in 5% H_3PO_4} was mixed with 100 μL of each supernatant. The absorbance of each solution was measured at 540 nm using a spectrophotometer (Bio-Rad, Hercules, CA, USA). The nitrite concentration was determined by comparison with a sodium nitrite standard curve. The percentage inhibition was calculated by the equation [1 − (NO level of test samples/NO level of vehicle-treated control)] × 100. The 50% inhibitory concentration (IC_{50}) was calculated from a nonlinear regression analysis (% inhibition versus concentration). L-NMMA was used as a positive control.

2.5. Cytotoxicity Assay

Cell viability was performed using the EZ-Cytox cell viability assay kit (DAEIL Lab, Seoul, Korea). The cells were seeded into 96-well plates at a density of 2×10^5 cells/mL, then incubated at 37 °C for 24 h. The cells were treated with two concentrations of compounds (20 and 40 μM) for an additional 24 h. After the 24 h incubation, 10 μL EZ-Cytox solution of the cell viability assay kit was added to each well and incubated for another 4 h at 37 °C and 5% CO_2. The relative cell viability was determined by measuring the formazan production using a spectrophotometer (Bio-Rad, Hercules, CA, USA) at an absorbance of 480 nm with a reference wavelength of 650 nm.

2.6. Statistical Analysis

All experiments were replicated at least three times to obtain means and standard deviations. Statistical significance was determined with analysis of variance using the multiple comparisons method of one-way ANOVA with Tukey's post hoc test using Prism 5.0 (GraphPad Software, Inc., San Diego, CA, USA). *p*-Values less than 0.05 indicated statistical significance. If a treatment effect was determined to be significant, Duncan's multiple range tests ($n = 3$) were performed to distinguish the means.

3. Results

3.1. Structure Identification of the Isolated Compounds

Since the ethyl acetate-soluble fraction of the hulls of *T. aestivum* (50 μg/mL) showed a NO production inhibitory activity of 62.11% in LPS-stimulated RAW 264.7 cells, it was subjected to phytochemical investigation. As a result, eight known compounds **1**–**8** were isolated and their structures were identified as tricin (**1**) [24], tricin 4′-*O*-[*threo*-*β*-guaiacyl-(7″-*O*-methyl-9″-*O*-acetyl)-glyceryl] ether (**2**) [25], tricin 4′-*O*-[*erythro*-*β*-guaiacyl-(7″-*O*-methyl-9″-*O*-acetyl)-glyceryl] ether (**3**) [25], tricin 4′-*O*-[*threo*-*β*-guaiacyl-(9″-*O*-acetyl)-glyceryl] ether (**4**) [25,26], tricin 4′-*O*-[*threo*-*β*-guaiacyl -(7″-*O*-methyl)-glyceryl] ether (**5**) [27], tricin 4′-*O*-[*erythro*-*β*-guaiacyl-(7″-*O*-methyl)-glyceryl] ether (**6**) [27], tricin 4′-*O*-[*threo*-*β*-4″-hydroxyphenyl-(7″-*O*-methyl)-glyceryl] ether (**7**) [28], and tricin 4′-*O*-[*erythro*-*β*-4″-hydroxyphenyl-(7″-*O*-methyl)-glyceryl] ether (**8**) [28], via the analysis of their spectroscopic data as well as the comparison of their data with published values (Figure 1).

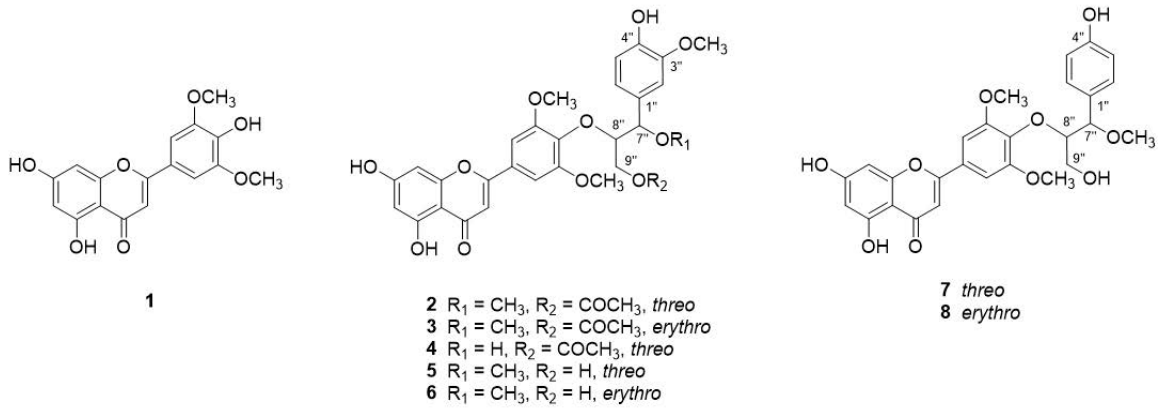

Figure 1. The chemical structures of **1**–**8** isolated from *T. aestivum* hull.

The relative stereochemistry of **2**-**8** was determined by a coupling constant (*J*) between H-7″ and H-8″. In the ^{1}H NMR spectra of **2**-**4** (in acetone-d_4), the large $J_{\text{H-7″,H-8″}}$ value (6.3 and 6.7 Hz, respectively) of compounds **2** and **4** indicated a *threo* configuration, whereas the small $J_{\text{H-7″,H-8″}}$ value (4.8 Hz) of compound **3** suggested an *erythro* configuration. In the ^{1}H NMR spectra of **5**-**8** (in acetone-d_4), the coupling constant of **5** and **7** showed a larger $J_{\text{H-7″,H-8″}}$ value (6.7 and 6.8 Hz, respectively) than those of **6** and **8** (6.2 and 6.4 Hz, respectively), providing the 7″,8″-*threo*-configuration for **5** and **7** and the 7″,8″-*erythro*-configuration for **6** and **8**. In addition, we also observed that the resonance for the methylene protons (H-9″a and H-9″b) in the ^{1}H NMR spectra of the *threo* type was shifted to upfield, compared to the corresponding proton signals in the *erythro* type. Most previous stereochemical studies of similar flavonolignans have reported their relative configurations [24–27,29,30]. Although CD experiments could be suggested to establish the absolute configuration of the flavonolignans, the isolates **2**-**8** did not exhibit CD Cotton effects in our study. This phenomenon may be explained by their conformational mobility, as described in a previous study [31]. The CD spectrum depends on the weighted average of the spectra of all the conformers present in solution; there could thus appear different signs of the rotational intensity of a given transition. Therefore, it seems possible that the CD spectra of **2**–**8** were not observed, cancelling their overlapping spectra [32].

3.2. Chemotaxonomic Significance

Flavonolignans, consisting of a flavone, tricin, and a lignin (phenylpropanoid), guaiacyl or *p*-coumaryl moiety have been found in some species of plant families [33], namely Poaceae (*Sasa* [25], *Zizania* [27], *Oryza* [34–37], *Avena* [31], *Zea* [38], *Sorghum* [39], *Saccharum* [40–42], *Hyparrhenia* [29], or *Vetiveria* species [43]), Arecaceae (*Calamus* species) [30,44], and Chenopodiaceae (*Salsola* species) [45]. However, the occurrence of tricin-lignan-type compounds in *Triticum* species is reported for the first

time in this study. The isolation of compounds **2-8** from *T. aestivum* provides new chemotaxonomic information. Compounds **2-4** have been isolated from *Sasa veitchii* leaves as new compounds [25]; subsequently, **2** and **4** were also found in *Pyrus ussuriensis* peels and leaves [46] and *S. borealis* leaves, respectively [26]. The isolation of compounds **5** and **6** have been reported in several studies, i.e., **5** and **6** from *Zizania latifolia* [27], *Elymus natans* [28], *Arenaria kansuensis* [47], *Taraxacum officinale* [48]; **5** from *P. ussuriensis* [46] and *Lepidium meyenii* [24]; and **6** from *Oryza sativa* [34]. Compounds **7** and **8** were reported previously only as the constituents of *E. natans* [28]. Therefore, the discovery of tricin-lignans **2**–**8** in *Triticum* species may serve as a chemotaxonomic marker for that species.

3.3. Evaluation of the Biological Effects of the Isolates from the Hulls of T. aestivum

All compounds were evaluated for their anti-inflammatory activities and cell viabilities in LPS-induced RAW 264.7 macrophage cells. The LPS treatment markedly increased NO production in RAW 264.7 cells compared with that in the control cells, whereas the **1**–**4** and **6**–**8** pretreatment inhibited NO production in a concentration-dependent manner (Figure 2). We could not observe any NO production reduction in the case of **5**. All compounds except for **4** exhibited no obvious cytotoxicity at 40 μM; however, **4** showed slight toxicity. These results are shown in Table 1. In the structures of **2**–**4** in which the *O*-acetyl group was substituted to C-9″, **2** and **4** with 7″,8″-*threo*-configuration inhibited NO production at lower inhibitory concentrations than the *erythro* type of **3**. However, in the structures of **5**–**8** in which the hydroxy group was substituted to C-9″, **6** and **8** with 7″,8″-*erythro*-configuration were more effective than the *threo* types of **5** and **8**. Therefore, it is expected that the substituents at C-9″ and the stereochemistry of C-7″ and C-8″ influence the activity of the compounds. Among the tested compounds, two compounds (**4** and **6**) showing IC_{50} values less than 40 μM were considered as active components of the *T. aestivum* hull for targeting inflammation-related diseases. However, in order to verify the potential benefit of **4** and **6** as an anti-inflammatory agent, further mechanism and in vivo inflammation disease studies are required.

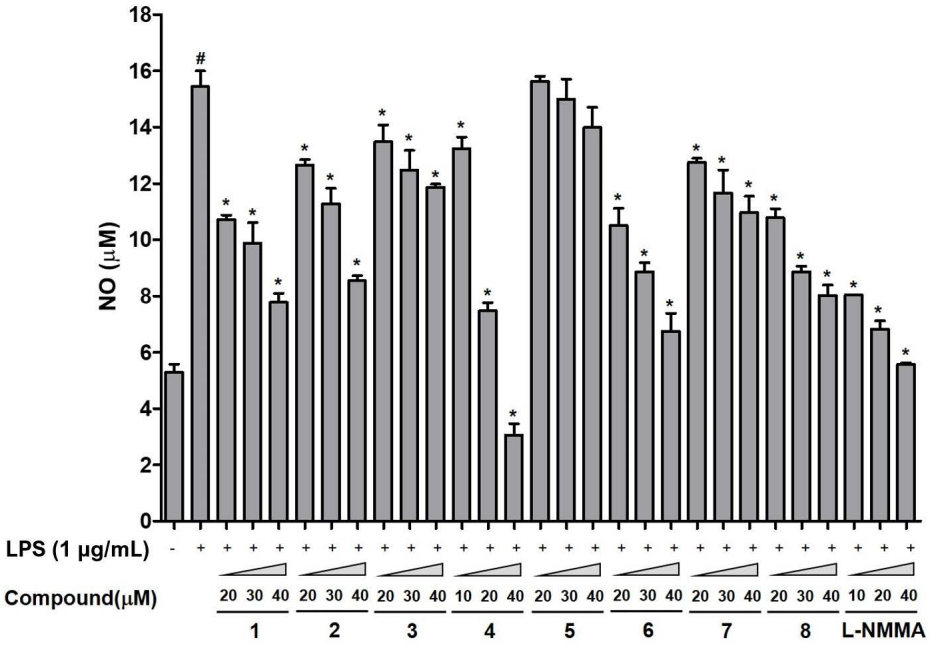

Figure 2. The effects of **1-8** on NO production in RAW 264.7 cells. The values are expressed as the mean ± SD of three independent experiments. $^{\#}$ $p < 0.05$ vs. negative control. * $p < 0.05$ vs. the group treated with LPS only.

Table 1. Inhibitory effects of the compounds **1**-**8** on the LPS-induced NO production in RAW 264.7 cells.

Compounds	IC_{50} (μM)	Cell Viability (%) [1]
1	46.41	>100
2	58.95	99.7 ± 2.1
3	>100	99.3 ± 2.3
4	24.14	85.7 ± 4.0
5	>100	98.8 ± 3.2
6	37.52	>100
7	>100	99.8 ± 10.8
8	45.67	>100
L-NMMA [2]	51.01	>100

[1] The cell viability after treatment with 40 μM compounds. [2] L-NMMA was used as the positive control.

Anti-inflammatory compounds have been discovered in natural products [49,50]. The laboratory models for anti-inflammatory screening of naturally occurring compounds are important tools for discovering drug candidates related to various inflammations [51]. To the best of our knowledge, our study is the first report evaluating the anti-inflammatory activities of compounds **2**–**4**, **7**, and **8**, even though compounds **1**, **5**, and **6** have been reported to exhibit inhibitory effects on LPS-induced nitrite or NO production in RAW 264.7 cells [24,27,34,48]. In particular, **5** has inhibited NO production with an IC_{50} of 10.8 μM [34] and has shown 43.76% inhibition at a concentration of 10 μg/mL [27] or 64.0% inhibition at 20 μg/mL [24] in the previous reports. However, its inhibitory activity was not observed in this study. In addition, there have been reports that **2** and **5** exhibited DPPH scavenging activities [45] and **5**–**8** showed phytotoxic effects against plant seedlings [28]. However, **3** and **4** have never been associated with any biological activity.

4. Conclusions

The current phytochemical research on wheat hull began with a shift in perception of wheat waste. Because wheat is one of the world's major crops, the quantity of by-products is also considerable. Therefore, studies reevaluating this common agricultural waste were considered as potential for research into new resources that have not yet been explored.

The bioassay-guided investigation of the active ethyl acetate fraction of *T. aestivum* hull afforded eight compounds, namely a typical cereal flavone, tricin (**1**), and seven flavonolignans (**2**–**8**). Flavonolignans **2**–**8** have not yet been isolated from *Triticum* species. The presence of the flavonolignans in wheat is supported by previous studies reporting the use of tricin in grass lignification, but these findings serve as new chemotaxonomic information for *Triticum* species.

In addition, this is the first report on the evaluation of flavonolignans **2**–**4**, **7**, and **8** on NO production inhibitory activities in LPS-stimulated RAW 264.7 macrophage cells. Among tested compounds, **4** and **6** were demonstrated as effectively inhibiting LPS-induced NO production. Excess NO production has been reported to cause inflammatory diseases, and the evaluation of inhibitory effects on NO production has been developed as an in vitro research model to find lead compounds for potential anti-inflammatory agents. Thus, the present results provide experimental evidence for the medicinal benefit of *T. aestivum* hull in the treatment of inflammatory diseases.

Supplementary Materials: The following are available online at http://www.mdpi.com/2076-3417/10/23/8656/s1, Table S1: Reported constituents of the aerial, hull, bran, and sprout part of *T. aestivum*, Figure S1: The chemical structures of reported constituents of the aerial, hull, bran, and sprout part of *T. aestivum*, Figures S2–S16: ^{1}H and ^{13}C NMR spectra of compounds **1**–**8**.

Author Contributions: Conceptualization, A.-R.H., M.J.H., and C.H.J.; methodology, A.-R.H., M.J.H., C.H.J., and J.-W.N.; software, A.-R.H., Y.-S.K., and H.H.P.; validation, A.-R.H., C.H.J., and J.-W.N.; formal analysis, A.-R.H., Y.-S.K., and H.H.P.; investigation, A.-R.H., Y.-S.K., J.P., and H.H.P.; resources, M.J.H. and J.-B.K.; data curation, A.-R.H., Y.-S.K., and H.H.P.; writing—original draft preparation, A-R.H. and Y.-S.K.; writing—review and editing, A-R.H., Y.-S.K., J.P., and J.-W.N.; visualization, A.-R.H., Y.-S.K., and C.H.J.; supervision, J.-W.N.

and J.-B.K.; project administration, C.H.J. and J.-B.K.; funding acquisition, C.H.J. and J.-B.K. All authors have read and agreed to the published version of the manuscript.

Funding: This research was supported by the Radiation Technology R&D program (grant number 2017M2A2A6A05018541) through the National Research Foundation of Korea (NRF) funded by the Ministry of Science, ICT & Future Planning.

Acknowledgments: The authors thank the Core Research Support Center for Natural Products and Medical Materials (CRCNM), Gyeongsangbuk-do, Gyeongsan-si, Korea, for technical support for NMR and CD experiments.

Conflicts of Interest: The authors declare no conflict of interest.

References

1. Adom, K.K.; Sorrells, M.E.; Liu, R.H. Phytochemicals and antioxidant activity of milled fractions of different wheat varieties. *J. Agric. Food Chem.* **2005**, *53*, 2297–2306. [CrossRef]
2. Liu, R.H. Whole grain phytochemicals and health. *J. Cereal Sci.* **2007**, *46*, 207–219. [CrossRef]
3. Hong, M.J.; Kim, D.Y.; Nam, B.M.; Ahn, J.-W.; Kwon, S.-J.; Seo, Y.W.; Kim, J.-B. Characterization of novel mutants of hexaploid wheat (*Triticum aestivum* L.) with various depths of purple grain color and antioxidant capacity. *J. Sci. Food Agric.* **2019**, *99*, 55–63. [CrossRef] [PubMed]
4. Zhu, Y.; Sang, S. Phytochemicals in whole grain wheat and their health-promoting effects. *Mol. Nutr. Food Res.* **2017**, *61*, 1600852. [CrossRef] [PubMed]
5. Deroover, L.; Tie, Y.; Verspreet, J.; Courtin, C.M.; Verbeke, K. Modifying wheat bran to improve its health benefits. *Crit. Rev. Food Sci. Nutr.* **2020**, *60*, 1104–1122. [CrossRef]
6. Budhwar, S.; Chakraborty, M.; Sethi, K.; Chatterjee, A. Antidiabetic properties of rice and wheat bran—A review. *J. Food Biochem.* **2020**, *44*, e13424. [CrossRef]
7. Arun, K.B.; Dhanya, R.; Chandran, J.; Abraham, B.; Satyan, S.; Nisha, P. A comparative study to elucidate the biological activities of crude extracts from rice bran and wheat bran in cell line models. *J. Food Sci. Technol.* **2020**, *57*, 3221–3231. [CrossRef]
8. Lee, J.Y.; Ahn, E.-K.; Park, J.-H.; Oh, J.S. Wheat bran extract regulates mast cell-mediated allergic responses in vitro and in vivo. *Molecules* **2020**, *25*, 3997. [CrossRef]
9. Bledzki, A.K.; Mamun, A.A.; Bonnia, N.N.; Ahmad, S. Basic properties of grain by-products and their viability in polypropylene composites. *Ind. Crops Prod.* **2012**, *37*, 427–434. [CrossRef]
10. Kowalska, I.; Pecio, L.; Ciesla, L.; Oleszek, W.; Stochmal, A. Isolation, chemical characterization, and free radical scavenging activity of phenolics from *Triticum aestivum* L. aerial parts. *J. Agric. Food Chem.* **2014**, *62*, 11200–11208. [CrossRef]
11. Zhu, Y.; Soroka, D.; Sang, S. Oxyphytosterols as active ingredients in wheat bran suppress human colon cancer cell growth: Identification, chemical synthesis, and biological evaluation. *J. Agric. Food Chem.* **2015**, *63*, 2264–2276. [CrossRef]
12. Moheb, A.; Grondin, M.; Ibrahim, R.K.; Roy, R.; Sarhan, F. Winter wheat hull (husk) is a valuable source for tricin, a potential selective cytotoxic agent. *Food Chem.* **2013**, *138*, 931–937. [CrossRef]
13. Hong, S.S.; Oh, J.S. Inhibitors of antigen-induced degranulation of RBL-2H3 cells isolated from wheat bran. *J. Korean Soc. Appl. Biol. Chem.* **2012**, *55*, 69–74. [CrossRef]
14. Luyen, B.T.T.; Thao, N.P.; Tai, B.H.; Lim, J.Y.; Ki, H.H.; Kim, D.K.; Lee, Y.M.; Kim, Y.H. Chemical constituents of *Triticum aestivum* and their effects on adipogenic differentiation of 3T3-L1 preadipocytes. *Arch. Pharm. Res.* **2015**, *38*, 1011–1018. [CrossRef] [PubMed]
15. Poudel, B.; Nepali, S.; Xin, M.; Ki, H.-H.; Kim, Y.-H.; Kim, D.-K.; Lee, Y.-M. Flavonoids from *Triticum aestivum* inhibit adipogenesis in 3T3-L1 cells by upregulating the insig pathway. *Mol. Med. Rep.* **2015**, *12*, 3139–3145. [CrossRef] [PubMed]
16. Moncada, S.; Higgs, E.A. Molecular mechanisms and therapeutic strategies related to nitric oxide. *FASEB J.* **1995**, *9*, 1319–1330. [CrossRef] [PubMed]
17. Ohshima, H.; Bartsch, H. Chronic infections and inflammatory processes as cancer risk factors: Possible role of nitric oxide in carcinogenesis. *Mutat. Res.* **1994**, *305*, 253–264. [CrossRef]
18. Krönche, K.D.; Fensel, K.; Kolb-Bachofen, V. Inducible nitric oxide synthase in human diseases. *Clin. Exp. Immunol.* **1998**, *113*, 147–156. [CrossRef]
19. Nathan, C.; Xie, Q.W. Regulation of biosynthesis of nitric oxide. *J. Biol. Chem.* **1994**, *269*, 13725–13728.

20. Hobbs, A.J.; Higgs, A.; Moncada, S. Inhibition of nitric oxide synthase as a potential therapeutic target. *Annu. Rev. Pharmacol. Toxicol.* **1999**, *39*, 191–220. [CrossRef]
21. MacMicking, J.; Xie, Q.W.; Nathan, C. Nitric oxide and macrophage function. *Annu. Rev. Immunol.* **1997**, *15*, 323–350. [CrossRef] [PubMed]
22. Coleman, J.W. Nitric oxide in immunity and inflammation. *Int. Immunopharmacol.* **2001**, *1*, 1397–1406. [CrossRef]
23. Zamora, R.; Vodovotz, Y.; Billiar, T.R. Inducible nitric oxide synthase and inflammatory diseases. *Mol. Med.* **2000**, *6*, 347–373. [CrossRef] [PubMed]
24. Bai, N.; He, K.; Roller, M.; Lai, C.-S.; Bai, L.; Pan, M.-H. Flavonolignans and other constituents from *Lepidium meyenii* with activities in anti-inflammation and human cancer cell lines. *J. Agric. Food Chem.* **2015**, *63*, 2458–2463. [CrossRef]
25. Nakajima, Y.; Yun, Y.S.; Kunugi, A. Six new flavonolignans from *Sasa veitchii* (Carr.) Rehder. *Tetrahedron* **2003**, *59*, 8011–8015. [CrossRef]
26. Jeong, Y.H.; Lee, J.; Kwon, Y.J.; Seo, E.K. Reverse-phase HPLC method for identification of diastereomeric constituents from *Sasa Boreal*. *Yakhak Hoeji* **2006**, *50*, 21–25.
27. Lee, S.-S.; Baek, Y.-S.; Eun, C.-S.; Yu, M.-H.; Baek, N.-I.; Chung, D.-K.; Bang, M.-H.; Yang, S.-A. Tricin derivatives as anti-inflammatory and anti-allergic constituents from the aerial part of *Zizania latifolia*. *Biosci. Biotechnol. Biochem.* **2015**, *79*, 700–706. [CrossRef]
28. Liu, Q.; Wu, C.; Peng, A.; Gao, K.; Che, J.; Li, Y.; Fu, H. Flavonolignans from *Elymus natans* L. and phytotoxic activities. *J. Agric. Food Chem.* **2017**, *65*, 1320–1327. [CrossRef]
29. Bouaziz, M.; Veitch, N.C.; Grayer, R.J.; Simmonds, M.S.J.; Damak, M. Flavonolignans from *Hyparrhenia hirta*. *Phytochemistry* **2002**, *60*, 515–520. [CrossRef]
30. Chang, C.-L.; Wang, G.-J.; Zhang, L.-J.; Tsai, W.-J.; Chen, R.-Y.; Wu, Y.-C.; Kuo, Y.-H. Cardiovascular protective flavonolignans and flavonoids from *Calamus quiquesetinervius*. *Phytochemistry* **2010**, *71*, 271–279. [CrossRef]
31. Wenzig, E.; Kunert, O.; Ferreira, D.; Schmid, M.; Schühly, W.; Bauer, R.; Hiermann, A. Flavonolignans from *Avena sativa*. *J. Nat. Prod.* **2005**, *68*, 289–292. [CrossRef] [PubMed]
32. Harada, N.; Sato, H.; Nakanishi, K. Configurational and conformational studies of sugars by the aromatic chirality method. *J. Chem. Soc. Chem. Commun.* **1970**, 1691–1693. [CrossRef]
33. Li, M.; Pu, Y.; Yoo, C.G.; Ragauskas, A.J. The occurrence of tricin and its derivatives in plants. *Green Chem.* **2016**, *18*, 1439. [CrossRef]
34. Jeong, R.-H.; Lee, D.-Y.; Cho, J.-G.; Lee, S.-M.; Kang, H.-C.; Seo, W.-D.; Kang, H.-W.; Kim, J.-Y.; Baek, N.-I. A new flavonolignan from the aerial parts of *Oryza sativa* L. inhibits nitric oxide production in RAW 264.7 macrophage cells. *J. Korean Soc. Appl. Biol. Chem.* **2011**, *54*, 865–870. [CrossRef]
35. Mohanlal, S.; Maney, S.K.; Santhoshkumar, T.R.; Jayalekshmy, A. Tricin 4′-*O*-(*erythro*-*β*-guaiacylglyceryl) ether and tricin 4′-*O*-(*threo*-*β*-guaiacylglyceryl) ether isolated from Njavara (*Oryza sativa* L. var. Njavara), induce apoptosis in multiple tumor cells by mitochondrial pathway. *J. Nat. Med.* **2013**, *67*, 528–533. [CrossRef]
36. Mohanlal, S.; Parvathy, R.; Shalini, V.; Helen, A.; Jayalekshmy, A. Isolation, characterization and quantification of tricin and flavonolignans in the medicinal rice Njavara (*Oryza sativa* L.), as compared to staple varieties. *Plant. Foods Hum. Nutr.* **2011**, *66*, 91–96. [CrossRef] [PubMed]
37. Dong, X.; Chen, W.; Wang, W.; Zhang, H.; Liu, X.; Luo, J. Comprehensive profiling and natural variation of flavonoids in rice. *J. Integr. Plant Biol.* **2014**, *56*, 876–886. [CrossRef]
38. Jung, Y.-J.; Park, J.-H.; Cho, J.-G.; Seo, K.-H.; Lee, D.-S.; Kim, Y.-C.; Kang, H.-C.; Song, M.-C.; Baek, N.-I. Lignan and flavonoids from the stems of *Zea mays* and their anti-inflammatory and neuroprotective activities. *Arch. Pharm. Res.* **2015**, *38*, 178–185. [CrossRef]
39. Huang, H.; Liu, Y.; Meng, Q.; Wei, S.; Cui, H.; Zhang, C. Flavonolignans and other phenolic compounds from *Sorghum halepense* (L.) Pers. *Biochem. Syst. Ecol.* **2010**, *38*, 656–658. [CrossRef]
40. Colombo, R.; Yariwake, J.H.; Queiroz, E.F.; Ndjoko, K.; Hostettmann, K. On-line identification of sugarcane (*Saccharum officinarum* L.) methoxyflavones by liquid chromatography–UV detection using post-column derivatization and liquid chromatography–mass spectrometry. *J. Chromatogr. A* **2005**, *1082*, 51–59. [CrossRef]
41. Colombo, R.; Yariwake, J.H.; Queiroz, E.F.; Ndjoko, K.; Hostettmann, K. On-line identification of further flavone C- and O-glycosides from sugarcane (*Saccharum officinarum* L., Gramineae) by HPLC-UV-MS. *Phytochem. Anal.* **2006**, *17*, 337–343. [CrossRef] [PubMed]

42. Bottcher, A.; Cesarino, I.; dos Santos, A.B.; Vicentini, R.; Mayer, J.L.S.; Vanholme, R.; Morreel, K.; Goeminne, G.; Moura, J.C.M.S.; Nobile, P.M. Lignification in sugarcane: Biochemical characterization, gene discovery, and expression analysis in two genotypes contrasting for lignin content. *Plant Physiol.* **2013**, *163*, 1539–1557. [CrossRef] [PubMed]
43. Gao, G.-C.; Lu, Z.-X.; Xu, H.-X.; Zheng, X.-S.; Yang, Y.-J. Chemical constituents from the aerial parts of *Vetiveria zizanioides*, *Chem. Nat. Compd.* **2012**, *48*, 128–129. [CrossRef]
44. Chang, C.-L.; Zhang, L.-J.; Chen, R.-Y.; Wu, C.-C.; Huang, H.-C.; Roy, M.C.; Huang, J.-P.; Wu, Y.-C.; Kuo, Y.-H. Quiquelignan A–H, eight new lignoids from the rattan palm *Calamus quiquesetinervius* and their antiradical, anti-inflammatory and antiplatelet aggregation activities. *Bioorga. Med. Chem.* **2010**, *18*, 518–525. [CrossRef] [PubMed]
45. Qiu, D.; Guo, J.; Yu, H.; Yan, J.; Yang, S.; Li, X.; Zhang, Y.; Sun, J.; Cong, J.; He, S.; et al. Antioxidant phenolic compounds isolated from wild *Pyrus ussuriensis* Maxim. fruit peels and leaves. *Food Chem.* **2018**, *15*, 182–187. [CrossRef] [PubMed]
46. Cui, Y.; Shao, Y.; Wang, Q.; Mei, L.; Tao, Y. Purification of flavonolignan diastereoisomers from *Arenaria kansuensis* by two-dimensional liquid chromatography combined with solid-phase extraction. *J. Chromatogr. Sci.* **2019**, *57*, 418–425. [CrossRef]
47. Choi, J.; Yoon, K.D.; Kim, J. Chemical constituents from *Taraxacum officinale* and their α-glucosidase inhibitory activities. *Bioorg. Med. Chem. Lett.* **2018**, *28*, 476–481. [CrossRef]
48. Kang, B.-M.; An, B.-K.; Jung, W.-S.; Jung, H.-K.; Cho, J.-H.; Cho, H.-W.; Jang, S.J.; Yun, Y.B.; Kuk, Y.I. Anti-inflammatory effect of tricin isolated from *Alopecurus aequalis* Sobol on the LPS-induced inflammatory response in RAW 264.7 cells. *Int. J. Mol. Med.* **2016**, *38*, 1614–1620. [CrossRef]
49. Gautam, R.; Jachak, S.M. Recent developments in anti-inflammatory natural products. *Med. Res. Rev.* **2009**, *29*, 767–820. [CrossRef]
50. Azab, A.; Nassar, A.; Azab, A.N. Anti-inflammatory activity of natural products. *Molecules* **2016**, *21*, 1321. [CrossRef]
51. Lau, T.A.; Bray, W.M.; Lokey, R.S. Macrophage cytological profiling and anti-Inflammatory drug discovery. *Assay Drug Dev. Technol.* **2019**, *17*, 14–16. [CrossRef] [PubMed]